3-D Simulation of the FCC Particle in Contact with an Oil Droplet at High Temperatures

Yang Ge, and L.-S. Fan
Department of Chemical and Biomolecular Engineering, The Ohio State University
Columbus, Ohio 43210

Abstract

A 3-dimensional numerical model is developed to simulate the process of collision between an evaporative droplet and a high temperature particle. This phenomenon is of direct relevance to many engineering process operations, such as fluid catalytic cracking (FCC), polyethylene synthesis, and electronic materials coating. In this study, the level-set method and the immersed-boundary method are combined to describe the droplet-particle contact dynamics in a fixed Eulerian grid. The droplet deformation is captured by one level-set function while the solid-fluid boundary condition is imposed on the particle surface through the immersed boundary method involving another level-set function. A 2-D vapor layer model is developed to simulate the vapor flow dynamics. Equations for the heat transfer characteristics are formulated for each of the solid, liquid and gas phases. The incompressible flow governing equations are solved using the finite volume method with the ALE (Arbitrary Lagrangian Eulerian) technique. The simulation results are validated through comparisons with experimental data obtained from the new experimental setup designed in this study. An important feature of the droplet impacting on a particle with film boiling is that the droplet undergoes a spreading, recoiling and rebounding process. Although the value for the maximum spread factor is larger for a higher impact velocity, the contact time is independent of the impact velocity. Both the normal collision and the oblique collision are considered in this study.

1. Introduction

Many engineering process operations involve the collision of liquid droplets with solid particles at high temperatures. In the petroleum industry, a fluid catalytic cracking (FCC) riser with an evaporative liquid jet is designed to provide effective liquid-solid contact and hence an increased rate of catalytic reactions in the riser. In the riser reactor, liquid hydrocarbon at a low temperature is injected from feed nozzles located at the bottom of the reactor, and the droplets formed from the spray are in contact with high-temperature fluidized catalyst particles (Fan, et al., 2001). The vaporized hydrocarbon then carries the catalyst particle up through the riser. In the feed nozzle region, the size of the formed droplet can be comparable or significantly larger than the size of the particle. With the droplets and particles of different sizes having different momentum at contact, the collision of the particles and the droplets may experience different contact modes (Zhu, et al., 2000). Smaller droplets may rebound from the surface of a larger particle upon impact due to the nature of the non-wetting contact. A smaller particle may penetrate or retain inside the larger droplet. Droplets may splash during the impact or remain attached to the particle surface after the collision and thereby intensify particle aggregation. Thus, understanding the droplet and particle contact mechanics is crucial to an accurate account of the momentum and heat transfer processes between the droplets and particles, and is important to the prediction of hydrocarbon product distributions in light of catalytic or thermal cracking reactions in the riser.

The droplet-particle collision processes in feed nozzle conditions are always accompanied by intense evaporation. In a FCC riser reactor, since the temperature of the catalytic particle is much larger than the saturation temperature of the oil droplet, the hydrocarbon vapor generated from evaporation forms a thin vapor layer which may prevent the direct contact of the droplet with the particle. Under this condition, the non-wetting contact may take place during the collision marking the film-boiling regime, or Leidenfrost regime (Gottfried, et al., 1966). A feature of the contact in the Leidenfrost regime is that the heat flux at the contact area is significantly smaller compared to that in the nucleate boiling regime and the transition-boiling regime, even though the temperature gradient across the vapor layer is higher. The vapor layer hinders the heat transfer from the solid to the droplet.

Extensive experiments were conducted to study the droplet impact on a flat surface under the film-boiling condition in the literature (e.g., Wachters and Westerling, 1966). The Weber number, defined by $We = \rho U_0^2 d_0 / \sigma$, was found to be able to characterize the droplet collision dynamics (Wachters and Westerling, 1966). The Leidenfrost temperature was determined as the temperature when the nonwetting contact occurs as the surface temperature increases (Chandra and Avedisian, 1991). The hydrocarbon droplet (n-heptane) was found to have a much lower transition temperature than the water droplet (Qiao and Chandra, 1996). When the surface temperature is above the Leidenfrost temperature of the liquid, the dynamics of the droplet were found to be independent of the surface materials (Hatta et al., 1997). The effects of the initial droplet temperature, which characterizes the subcooling degree of the droplet, on the behavior of the film-boiling impact were also reported (Inada, et al 1985; Chen and Hsu, 1995, Ge and Fan, 2005b).

Numerical simulations were performed to describe the droplet impingement onto isothermal flat wall (e.g., Mehdi-Nejad, 2003). In these simulations, the numerical techniques used to solve the moving interface problem generally related to two basic methods: the front tracking method and the front capturing method. The front tracking method includes the adaptive-grid finite element method (Fukai et al., 1995) and the immerse boundary method (IBM) (Francois and Shyy, 2003). In the front tracking method, the interface is explicitly described by a discrete set of markers or by a set of deformable structured mesh points. The interface motion is tracked by the advection of the Lagrangian markers in a flow field. The front capturing method, on the other hand, includes the volume of fluid (VOF) method (Pasandideh-Fard et al., 1998) and the level-set method (Zheng and Zhang, 2000). In the front capturing method, the moving front is implicitly represented by a scalar function defined on Eulerian mesh point. The advection equation of a scalar function, which represents the fluid volume fraction in the VOF method or the level-set function in the level set method, is solved to trace the interface movement. The interface force such as the surface tension force is incorporated in the flow momentum equation as a source term using the continuum surface force (CSF) method (Brackbill et al., 1992).

This study attempts to develop a three-dimensional model based on the level-set approach and the immersed boundary method to simulate the collision of a droplet with a superheated particle in the film boiling condition. The free surface of the deformable droplet and the rigid surface of the solid particle are both captured by two level-set functions in a fixed, regular Eulerian grid. The immersed boundary method is applied to impose the solid-fluid boundary condition at the particle surface. The governing equations for the droplet and the

surrounding gas phase are solved utilizing the finite volume method with the ALE (Arbitrary Lagrangian Eulerian) technique. A 2D vapor layer model is developed on a boundary layer coordinate to simulate the vapor flow dynamics inside the micro-scale vapor layer between the droplet and the particle. The heat transfer equations for the gas phase and particle phase are solved by considering the energy balance at the solid-vapor and vapor-liquid interfaces. Experiments are also conducted to substantiate the model and the simulation results based on the model obtained in this study.

2. Experimental

The schematic diagram of the experimental setup is shown in Fig. 1. The main experimental apparatus consists of a syringe, blunt-point needles of size 17 gauge, 21 gauge and 27 gauge, brass solid particles of sizes 5.5 mm, 3.2 mm. The brass particle is heated on a heating plate with adjustable temperature settings. The syringe is covered with two layers of insulation to prevent external heating of the liquid from the plate heater. A high-speed camera capable of capturing 500 frames per second is used to record the droplet-particle collision process. Two light sources are used to illuminate the particle and droplet from both the front and the back. A light diffuser is placed in front of the back light source to provide soft background lighting. A state-of-the-art fast-response type T thermocouple constructed from mineral insulated cable of 0.15 mm with a response time of 2 ms is inserted from the bottom and through the center of the particle to the particle surface. The fast response time for the thermocouple is crucial to the measurement of the rapid temperature change on the particle surface, which is at a time scale of ~10 ms, during the collision process. Different sizes of the droplet are formed by different needle sizes of the syringe. Small droplet sizes can also be formed with the aid of acoustic forces. By changing the height of the syringe, a wide range of *We* (10 – 200) for both the normal and oblique collisions can be established. Based on the photographs, the droplet-particle contact area and the droplet height relative to the particle are measured.

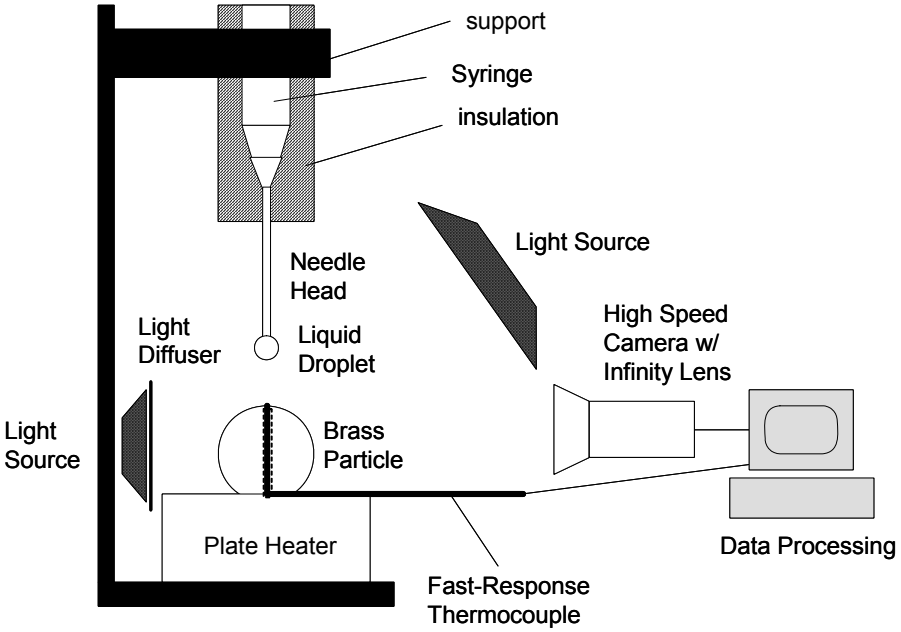

Figure 1. Schematic diagram of the experimental setup

3. Mathematical Model

The equations of conservation of mass and momentum for this 3-phase flow system can be given by:

$$\nabla \cdot \vec{V} = 0 \tag{1}$$

$$\rho(\frac{\partial \vec{V}}{\partial t} + \nabla \cdot \vec{V}\vec{V}) = -\nabla p + \rho\vec{g} + \nabla \cdot (2\mu\widetilde{D}) + \sigma\kappa(\phi_d)\delta(\phi_d)\nabla\phi_d + \vec{F}_p(\phi_p) + \vec{F}_{vapor} \tag{2}$$

where ϕ_d is the droplet level set function; $\vec{V}$ is the fluid velocity; $\rho = \rho(\phi_d)$ is the fluid density; $\mu = \mu(\phi_d)$ is the fluid viscosity; g is the gravitational acceleration; σ is the surface tension coefficient; and $\widetilde{D}$ is the stress tensor. The surface tension force is included in this model as a body force using the continuum surface model (CSM) (Brackbill et al., 1992). $\delta(\phi_d)$ is the one-dimensional delta function and $\kappa(\phi_d)$ is the curvature of the free surface defined as (Sussman, et al., 1998):

$$\kappa(\phi_d) = \nabla \cdot \frac{\nabla\phi_d}{|\nabla\phi_d|} \tag{3}$$

For the film boiling impact simulation, a micro-scale vapor layer model is required to determine the evaporation-induced pressure force $\vec{F}_{vapor}$ on both the droplet side and the moving particle side. Ge and Fan (2005a) developed a 2D model to simulate the dynamics of the vapor flow between the droplet and the flat surface considering the inertial force of the vapor. In this study, this model is extended to simulate the vapor flow within the particle-droplet contact area.

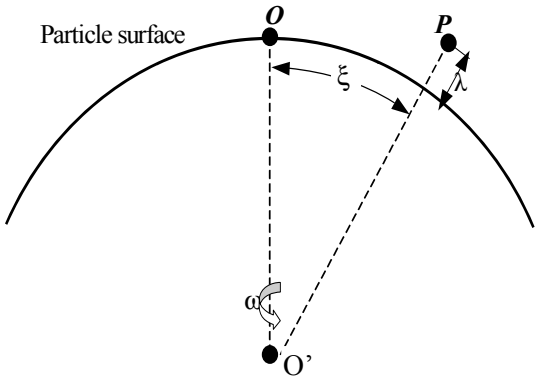

Figure 2. Boundary layer coordinates

As the vapor flows in the direction along the spherical surface of the particle, a boundary layer coordinate (ξ, λ, ω) given in Fig. 2 is employed to describe the vapor layer equation. In this coordinate, the Navier-Stocks equations for incompressible vapor flows with gravitation terms neglected are given by:

$$\frac{\partial u_\xi}{\partial \xi} + \frac{\cot(\xi/R)}{R}u_\xi + \frac{2}{R}u_\lambda + \frac{\partial u_\lambda}{\partial \lambda} = 0 \tag{4}$$

$$u_\xi\frac{\partial u_\xi}{\partial \xi} + u_\lambda\frac{\partial u_\xi}{\partial \lambda} + \frac{u_\xi u_\lambda}{R} = -\frac{\partial}{\partial \xi}(\frac{P}{\rho}) - \nu(\frac{\partial^2 u_\lambda}{\partial \xi \partial \lambda} - \frac{2}{R}\frac{\partial u_\xi}{\partial \lambda} - \frac{\partial^2 u_\xi}{\partial \lambda^2}) \tag{5}$$

$$u_\xi \frac{\partial u_\lambda}{\partial \xi} + u_\lambda \frac{\partial u_\lambda}{\partial \lambda} - \frac{u_\xi{}^2}{R} = -\frac{\partial}{\partial \lambda}(\frac{P}{\rho}) + \frac{\nu}{R}[R\frac{\partial^2 u_\lambda}{\partial \xi^2} - \frac{\partial u_\xi}{\partial \xi} - R\frac{\partial^2 u_\xi}{\partial \xi \partial \lambda} + \cot(\frac{\xi}{R})(\frac{\partial u_\lambda}{\partial \xi} - \frac{u_\xi}{R} - \frac{\partial u_\xi}{\partial \lambda})] \quad (6)$$

where u_ξ, u_λ are the vapor flow velocities in ξ and λ directions, respectively.

The heat transfer model is applied to calculate the temperature distribution inside the particle and in the gas phase. Inside the particle, the heat conduction equation is given by:

$$\frac{\partial T_s}{\partial t} = \alpha_s \nabla \cdot \nabla T_s \quad (7)$$

where α_s is the thermal diffusivity of particle. When the particle surface is in contact with the droplet through the vapor layer, the boundary condition at the particle surface is given by:

$$k_v \frac{T_{ps} - T_{ds}}{\delta} = -k_s \vec{n}_p \cdot \nabla_p T_s \quad (8)$$

where T_{ss}, T_{ds} are the interface temperatures of the particle and the droplet, respectively; k_v, k_s are the heat conductivity of the vapor phase and the solid particle, respectively; $\vec{n}_p$ is the normal vector of the particle surface, $\nabla_p T$ is the temperature gradient which is evaluated only on the particle side. Similar to the velocity interpolation at the particle surface, this boundary condition, Eq. (8), is imposed on the computational grid point, which is located in a small band (2ε) near the particle surface on the solid side. The temperatures defined at such grids are recalculated at each time step based on the temperature at the neighboring grid points to satisfy the boundary condition given by Eq. (8).

Since the thickness of the vapor layer is very thin, the temperature distribution in the vapor phase can be simplified to a 1-D equation in boundary layer coordinates:

$$\frac{\partial^2 T_v}{\partial \eta^2} = 0 \quad (9)$$

Neglecting the radiative heat transfer across the vapor layer, the energy balance equation on the liquid-vapor interface can be given as:

$$k_v \frac{T_{ps} - T_{ds}}{\delta} = -k_d \frac{\partial T_d}{\partial \eta} + \dot{m} L_c \quad (10)$$

where k_d is the thermal conductivity of the liquid droplet.

4. Sample Results

Sample results on experimental images and the simulated images are shown in Fig. 3. The figure describes the impact of a saturated acetone droplet of 2.1mm in diameter onto a 5.5mm particle at 250ºC. The impact velocity is 45 cm/s, which gives a Weber number of 12. The initial temperature of the droplet is at the saturated temperature of acetone (56ºC). The photos were taken using a high-speed camera. The mesh resolution of the simulation shown in Fig. 3 is 0.06mm in grid size, which gives a CPR (cell per droplet-radius) of 17.5. In the figure, the simulated 3D images of the droplet and particle are presented which show the iso-value surface at the position with zero droplet and particle level set functions. The time indicated in the figure starts at the instant of the collision. The figure shows that the droplet shape variations in the photos at various times are well reproduced by the simulation throughout the

entire collision process. The droplet undergoes spreading, recoiling and rebounding during the contact. For both the experiments and the simulation, the results show that during the first 5.5ms of the impact (0ms-5.5ms), a liquid film with a flattened disc shape is formed right after the collision. The liquid film then spreads out on the particle surface. This stage of droplet spreading is caused by the inertial force, which drives the liquid to flow out on the particle surface, until all the kinetic energy of the impact is either converted to the surface energy of the deformed droplet or dissipated by friction. The droplet film spreads to the maximum extent or about 7.5ms (frame 4), yielding a radius of droplet-particle contact area about 1.5 times that of the original radius of the droplet. The liquid film then starts to shrink back to its center (7.5ms-11.5ms) due to the surface tension force at the edge of the film. Beyond 11.5ms, the liquid film continues to recoil and forms an upward jet in the center of the droplet (11.5ms - 17.5ms), leading to the bouncing of the droplet up from the particle surface (21.5-27.5ms). The pignut-shape droplet shown in the photo at 21.5ms is reproduced in the simulation.

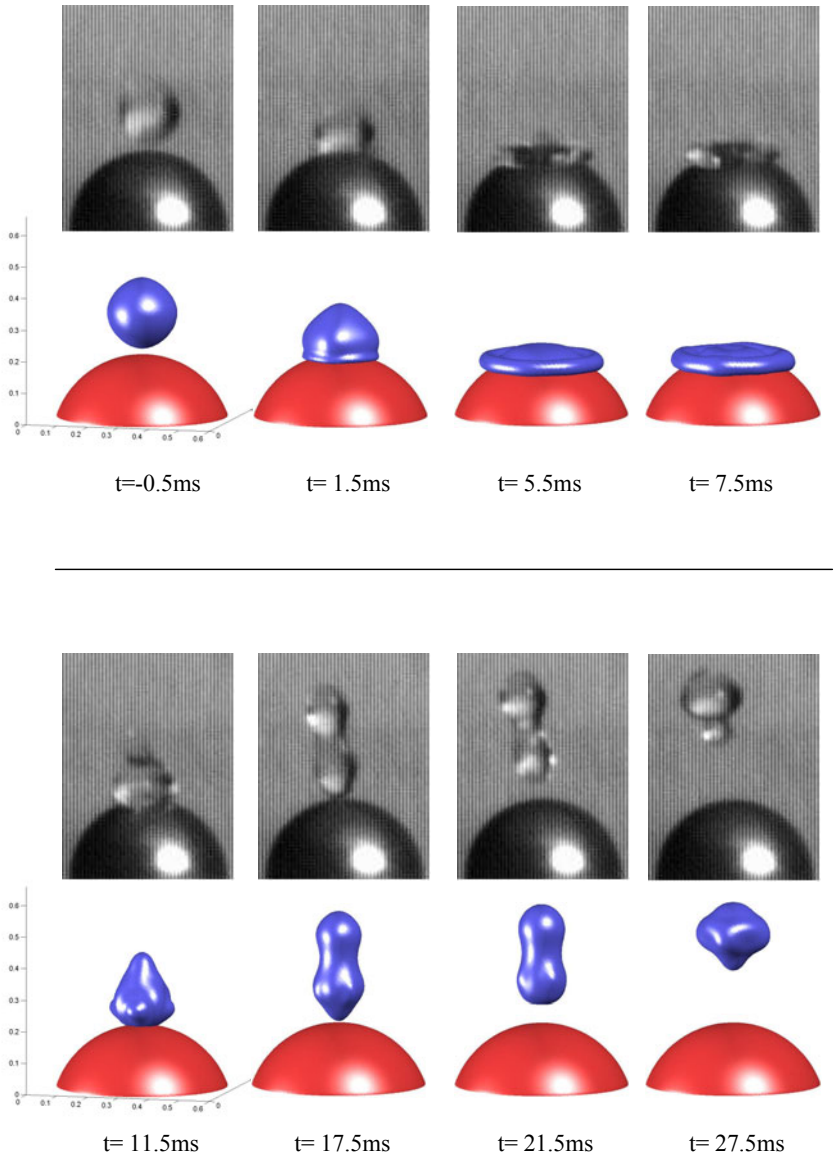

Figure 3. Experimental photos and simulated images of the 2.1mm acetone droplet impact on the 5.5mm particle at 250°C. The impact velocity is 45 cm/s. The unit for the coordinate is cm

5. Concluding Remarks

The 3-dimensional computational model developed in this study is capable of reproducing the droplet-particle collision process with significant heat transfer and phase change (evaporation). The level-set method and the immersed-boundary method are combined to describe the droplet-particle contact dynamics in the fixed Eulerian grid. The heat transfer properties in each phase are solved with a micro-scale vapor flow model, which is applied to determine the vapor pressure force during the contact process between the droplet and the superheated particle. The simulation reveals (not shown) that although a larger impact velocity gives a larger extent of the spreading, the contact time of the droplet on the particle surface is almost independent of the impact velocity. The heat fluxes on the particle surface reaches a higher level during the spreading process, and then sharply decreases during the recoiling process.

Nomenclature

Notations

D	Stress tensor
d	Diameter
F	Force
g	Gravitational acceleration
k	Heat conductivity
$\dot{m}$	Mass evaporation rate
p	Pressure
R	Radius
T	Temperature
t	Time
u	Velocity of the vapor flow
U	Particle velocity
$\boldsymbol{V}$	Fluid velocity
x	Position vector
We	Weber number

Greek Letters

α	Thermal diffusivity
Δ	Grid size
κ	Curvature of the surface
δ	δ function (or the thickness of the vapor layer)
ε	Thickness of the interface
ξ, λ	Coordinate defined in vapor layer model
η	$= \lambda/\delta$
ν	Kinematics Viscosity of vapor flow
ϕ	Level-set function
μ	Molecular viscosity
ρ	Density

σ Surface tension

Subscripts and superscripts

d droplet
g gas phase
l liquid phase
p particle
r radial direction
s solid
v vapor phase

References

Brackbill, J. U., Kothe, D. B., & Zemach, C. (1992). A continuum method for modeling surface tension. *Journal Comput. Phys., 100,* 335-354.

Chandra, S., & Avedisian, C. T. (1991). On the collision of a droplet with a solid surface. *Proc. R. Soc. Lond. A, 432,* 13-41.

Fan, L.-S., Lau, R., Zhu, C., Vuong, K., Warsito, W., Wang, X., & Liu, G. (2001). Evaporative liquid jets in gas-liquid-solid flow system. *Chem. Eng. Science, 56*, 5871-5891.

Francois, M., & Shyy, W. (2003). Computations of drop dynamics with the immersed boundary method, part1: numerical algorithm and buoyancy-induced effect. *Numerical Heat Transfer, Part B, 44,* 101-117.

Fukai, J., Shiiba, Y., Yamamoto, T., and Miyatake, O. (1995). Wetting effects on the spreading of a liquid droplet colliding with a flat surface: Experiment and modeling. *Physics of Fluids, 7(2)*, 236.

Ge, Yang, & Fan, L.-S. (2005a). Three-dimensional simulation of impingement of a liquid droplet on a flat surface in the Leidenfrost regime. *Physics of Fluids, 17, 027104.*

Gottfried, B. S., Lee, C. J., & Bell, K. J. (1966). The Leidenfrost phenomenon: film boiling of liquid droplets on a flat plate. *International Journal of Heat and Mass Transfer, 9*, 1167-1187.

Hatta, N., Fujimoto, H., Kinoshita, K., & Takuda, H. (1997). Experimental study of deformation mechanism of a water droplet impinging on hot metallic surface above the Leidenfrost temperature. *Journal of Fluids Eng., 119,* 692-699.

Inada, S., Miyasaka, Y. & Nishida, K (1985). Transient heat transfer for a water drop impinging on a heated surface. *Bulletin of JSME, 28*, 2675-2681.

Mehdi-Nejad, V., Mostaghimi, J., and Chandra, S. (2003). Air bubble entrapment under an impacting droplet. *Physics of Fluids, 15(1),* 173-183.

Pasandideh-Ford, M., Bhola, R., Chandra, S., and Mostaghimi, J. (1998). Deposition of tin droplets on a steel plate: simulation and experiments. *International Journal of Heat and Mass Transfer, 41*, 2929-2945.

Qiao, Y. M., & Chandra, S. (1996). Boiling of droplet on a hot surface in low gravity. *International Journal of Heat and Mass Transfer, 39(7),* 1379-1393.

Sussman, M., Smereka, P., & Osher, S. (1994). A level set approach for computing solutions to incompressible two-phase flow. *Journal of Computational Physics, 114,* 146-159.

Wachters, L. H. J., Bonne, H., & Nouhuis, H. J. (1966). The heat transfer from a hot horizontal plate to sessile water drops in the spheroidal state. *Chem. Eng. Science, 21,* 923-936.

Zheng, L. L., & Zhang, H. (2000). An adaptive level set method for moving-boundary problem: application to droplet spreading and solidification. *Numerical Heat Transfer, Part B, 37,* 437-454.

Zhu, C., Wang, X., & Fan, L.-S. (2000). Effect of Solids Concentration on Evaporative Liquid Jets in Gas-Solid Flows. *Powder Technology, 111,* 79-82.